Multichannel Restoration with Limited *A Priori* Information

Michael J. Vrhel, *Member, IEEE,* and Michael Unser, *Senior Member, IEEE*

***Abstract*—We introduce a method for multichannel restoration of images in which there is severely limited knowledge about the undegraded signal, and possibly the noise. We assume that we know the channel degradations and that there will be a significant noise reduction in a postprocessing stage in which multiple realizations are combined. This post-restoration noise reduction is often performed when working with micrographs of biological macromolecules. The restoration filters are designed to enforce a projection constraint upon the entire system. This projection constraint results in a system that provides an oblique projection of the input signal into the subspace defined by the reconstruction device in a direction orthogonal to a space defined by the channel degradations and the restoration filters. The approach achieves noise reduction without distorting the signal by exploiting the redundancy of the measurements.**

I. Introduction

MULTICHANNEL restoration problems occur in many image processing applications including color imaging, electron microscopy, and remote sensing [1]–[4]. Classically, the restoration problem is framed in the discrete domain which constrains the signals to be bandlimited. In addition, prior information is typically assumed to be available in the form of the original signal's power spectrum, higher order spectra, or constraining sets. In some applications, this information may be difficult to determine or estimate from the recorded data. A particular example occurs in electron microscopy, in which the exact structure of the object under examination may be unknown. This example has motivated us to consider the problem of multichannel restoration with limited prior information about the undegraded signal. The restoration problem is formulated in the continuous domain using notation similar to that described in [13]. This approach places no constraints on the input signal (e.g., bandlimitedness is not required) other than finite energy. Since our primary motivation for this work came from a problem in electron microscopy we will briefly describe where our approach fits into the overall problem of imaging biological macromolecules.

In electron microscopy, there exists a tradeoff between image contrast and the amount the image is in focus. As the image is brought into focus, its contrast decreases. For this reason, high-resolution electron micrographs are recorded with a significant amount of defocus. This results in a degradation that includes the complete loss of information at certain spatial frequencies (i.e., frequency nulls). Because the location of these frequency nulls is a function of the defocus setting, it is advisable to record multiple images of the same object at varying degrees of defocus [5].

To keep from damaging the specimen, high resolution electron micrographs of biological macromolecules are recorded at low electron doses. The use of a low electron dose produces an image with a low signal-to-noise ratio (SNR), typically on the order of 0 dB. In practice, the noise is reduced in a postprocessing phase, in which a large number of images of identical specimens are combined. In the simplest case, the macromolecules have a preferred three-dimensional (3-D) orientation and the different views of the specimen are combined by correlation averaging [6]. When the particles are randomly oriented, data reduction is achieved through 3-D reconstruction. This type of processing is much more challenging and is currently only applicable when the particles exhibit a very high degree of symmetry (e.g., icosahedral viruses) [7]. Such 3-D reconstructions provide extremely valuable structural information on viruses and there is currently a strong incentive for improving their resolution [8].

The situation is therefore one in which we have many noisy images of the same object (possibly at different orientations) for several focus settings. A block diagram of the entire process is shown in Fig. 1. Since there will be significant noise reduction in the combining of these multiple images, it is critical that the individual images are not overly smoothed in the restoration phase. Statistical multichannel deconvolution approaches such as Wiener filtering [2], [9], or Bayesian methods [10], [11] require prior information about the input signal, which may be difficult to obtain in practice, especially in a case such as electron microscopy in which a prototype image is not available. Without the correct signal statistics, the use of statistical methods can result in a distorted signal estimate [1], [11], [12]. In addition, the exact amount of noise reduction achieved in the postprocessing must be known for the statistical methods if significant smoothing is to be avoided. This information is difficult to determine due to the complexity of the iterative 3-D reconstruction algorithms that incorporate particle symmetry conditions and use an undetermined number of particles. In other words, it is often not known how many individual images will be used in the reconstruction until the reconstruction algorithm is completed. Another important consideration is that most statistical methods achieve noise reduction at the expense of some signal degradation. Many biological scientists are not comfortable with this idea. They would rather be presented with undistorted noisy data and rely on their own visual system for noise reduction.

Manuscript received November 20, 1996; revised May 5, 1998. The associate editor coordinating the review of this manuscript and approving it for publication was Prof. Stephen E. Reichenbach.

M. J. Vrhel is with Color Savvy Systems Ltd., Springboro, OH 45066 USA (e-mail: mvrhel@colorsavvy.com).

M. Unser is with the Biomedical Imaging Group, Swiss Federal Institute of Technology, CH-1015 Lausanne, Switzerland.

Publisher Item Identifier S 1057-7149(99)02468-9.

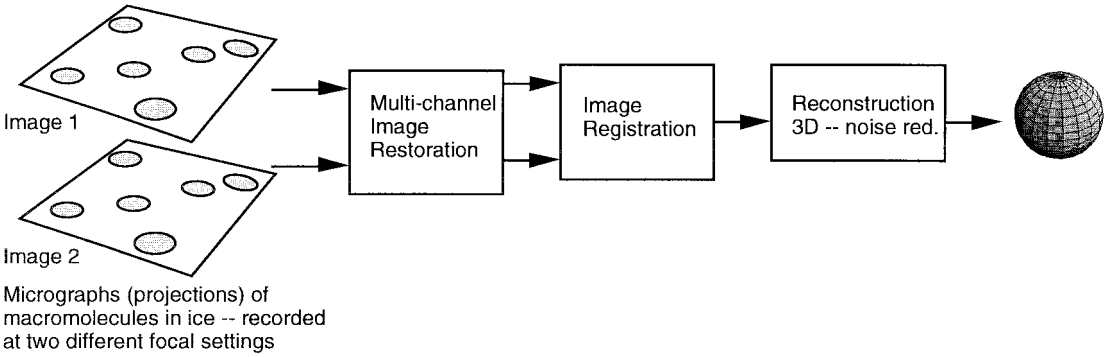

Fig. 1. Overview of multichannel restoration problem in electron microscopy application.

Our approach to this multichannel deconvolution problem is one which requires no prior information about the input signal. The method is a multichannel extension of the generalized sampling problem discussed in [13] and includes as a special case a current processing technique in electron microscopy [14]. The approach incorporates knowledge of the final reconstruction method, which can include splines, wavelets, or display devices. In addition, unlike most classical formulations the input signal is not required to be bandlimited; it can be an arbitrary finite energy function. The method enforces a system projection constraint which produces less smoothing of the signal than the statistical techniques, at the expense of less noise reduction. The projection constraint ensures no loss of signal information if the input signal is included in the reconstruction space (e.g., the class of bandlimited functions, cubic spline functions, etc.). The residual in such a case will consist of noise only. As already mentioned, these properties are particularly relevant for the restoration of electron micrographs.

The following mathematical notations are used in this paper.

L_2 is the space of measurable, square-integrable, real-valued functions.

l_2 is the vector space of square-summable sequences (or discrete signals).

$\langle g(x), f(x)\rangle = \int_{-\infty}^{+\infty} g(x)f(x)\,dx$ is the inner product operation in L_2.

The Fourier transform of a discrete 2-D signal $r(k,j)$ will be denoted by $R(u,v)$.

The paper is organized as follows. We will first describe the approach mathematically in Section II. Section III deals with the selection of weighting coefficients to minimize the noise residue in the restored image. In Section IV, we consider some practical implementation issues. Finally in Section V we conclude with simulations.

II. The Projection Constraint

A. Problem Formulation

Mathematically, the recording process for an N-channel system can be represented by

$$\begin{aligned} r_i(k,j) &= \langle \varphi_i(x-k, y-j), f(x,y)\rangle + n_i(k,j) \\ &= c_i(k,j) + n_i(k,j) \quad i = 1, \cdots N \end{aligned} \tag{1}$$

where $r_i(k,j)$ is the recorded data for channel i, $c_i(k,j)$ are idealized noise-free recorded values, $n_i(k,j)$ is signal independent additive noise, $f(x,y)$ is the continuous input, and $\varphi_i(-x,-y)$ is the impulse response in the ith channel. Note that in practice the only information available is $\varphi_i(-x,-y)$ and $r_i(k,j)$ $i = 1, \cdots, N$.

The goal is to reconstruct an estimate of the continuous signal $f(x,y)$ from the recorded values $r_i(k,j)$ $i = 1, \cdots, N$. We will achieve this goal by digital filtering and by a suitable reconstruction method. Fig. 2 contains a diagram of a two channel system which includes the measurement process and the restoration/reconstruction process. The q_i's are the digital restoration filters to be designed. The function $\varphi_0(x,y)$ defines the output signal subspace which we denote by

$$V_0 = \left\{ h(x,y) = \sum_j \sum_k \varphi_0(x-k, y-j)p(k,j) \,\middle|\, p(k,j) \in l_2 \right\}.$$

Note that this formulation of V_0 provides us with a discrete representation (via the samples $p(k,j)$) and a continuous model (via $h(x,y)$) of our output signal (V_0 is the space of all signals which can be decomposed in the above fashion). The integer translates of $\varphi_0(x-k, y-j)$ are a set of basis functions which define the output signal subspace. Typically, $\varphi_0(x,y) = \operatorname{sinc}(x)\operatorname{sinc}(y)$ (separable sinc) but our model is sufficiently general to include many other representations such as splines and wavelets [15]. Therefore, if $\varphi_0(x,y) = \operatorname{sinc}(x)\operatorname{sinc}(y)$, then all output signals produced by this system must be bandlimited. Note, however, that we have not placed any constraints on the input signal $f(x,y)$ (e.g., the signal need not be bandlimited) and if some other set of basis functions were selected to define V_0 (e.g., translations of a cubic spline), then the output signal would also not be bandlimited even though we are sampling and digitally filtering (cf. [13]).

The system output can be divided into two portions as shown in Fig. 2 where we have the output as the sum $\tilde{f}(x,y) + \tilde{n}(x,y)$. Since the system is linear, we can use $\tilde{f}(x,y)$ to represent that portion of the output caused by the input $f(x,y)$. The portion $\tilde{n}(x,y)$ then represents the output caused by the noise inputs $n_i(k,j)$ $i = 1, \cdots, N$. Similarly, the input to $\varphi_0(x,y)$ is divided between an input signal related portion $d_f(k,j)$ and a noise related portion $d_n(k,j)$.

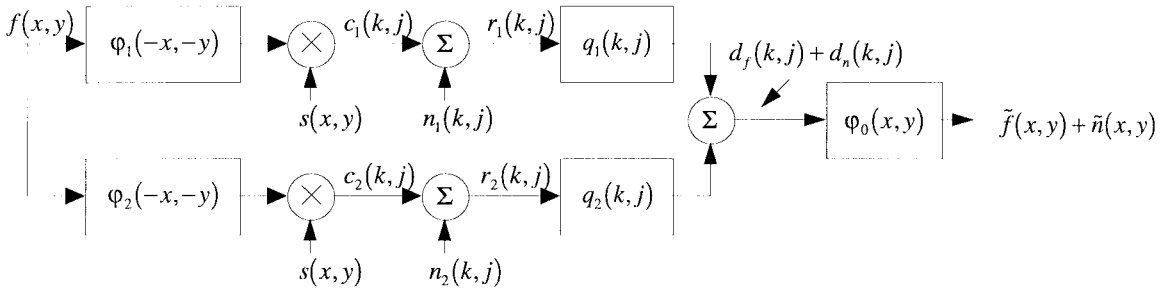

Fig. 2. Two-channel system where $s(x,y) = \sum_k \sum_j \delta(x-k, y-j)$.

The goal is to design the digital filters $q_i(k,j)\ i = 1, \cdots, N$, using no prior signal information such that if it is possible for the reconstruction process to reproduce $f(x,y)$ (that is if $f(x,y) \in V_0$), then $f(x,y) = \tilde{f}(x,y)$. In other words, we do not want to distort the nonnoise portion of the output if possible. With this requirement, designing the overall system (from $f(x,y)$ to $\tilde{f}(x,y)$ as shown in Fig. 2) to act as a projection operator becomes desirable. Specifically, if the system is a projection operator, then given that the input $f(x,y)$ satisfies $f(x,y) \in V_0$, the output portion $\tilde{f}(x,y)$ will be a perfect reconstruction of the input signal.

It is, of course, possible that the input $f(x,y)$ is not contained in V_0. This situation implies that our reconstruction method (through φ_0) cannot recreate the signal $f(x,y)$. In this case, the best solution, in the least squares sense, is the orthogonal projection of $f(x,y)$ onto V_0. Since $f(x,y)$ is not directly available (nor is any prior information about the signal), the least squares solution is difficult to obtain when $f(x,y) \notin V_0$. For such an input, our projection-based system provides, as an estimate, the projection of $f(x,y)$ onto V_0 in the direction orthogonal to a subspace defined by the input impulse responses and the filters $q_i(k,j)\ i = 1, \cdots, N$. This oblique projection provides consistency with the measured values which is the only information available about $f(x,y)$. By *consistency* we mean that if the output portion $\tilde{f}(x,y)$ (the nonnoise related portion of the output) were fed back into the input of the system, then we would obtain the same idealized noise-free values $c_i(k,j)\ i = 1, \cdots, N$ [cf. (1)] that were obtained when the input was $f(x,y)$.

At this point the only constraint that we have placed upon our system is that it must be a projection operator. A linear operator $P: L_2 \to V_0$ is a projection operator if it satisfies the following property:

$$\forall f \in V_0, \quad Pf = f.$$

The filters $q_i(k,j)\ i = 1, \cdots N$ are the parameters that we have available to achieve a system that is a projection operator onto V_0. Therefore, let us consider what general class of filters would provide us with an overall system (as shown in Fig. 2) that satisfies the above projection property.

B. Projection Constraint Formulation

A general signal $f(x,y) \in V_0$ can be decomposed as

$$f(x,y) = \sum_j \sum_k d(k,j)\varphi_0(x-k, y-j) \tag{2}$$

where $d(k,j) \in l_2$ are the discrete coefficients which describe $f(x,y)$ in V_0. The projection requirement implies

$$\tilde{f}(x,y) = f(x,y),$$

or equivalently

$$d(k,j) = d_f(k,j). \tag{3}$$

The sample values in channel i for the input $f(x,y)$ can be expressed by the inner product

$$\begin{aligned} c_i(k,j) &= \left\langle \sum_j \sum_k d(k,j)\varphi_0(x-k, y-j), \varphi_i(x-l, y-m) \right\rangle \\ &= \sum_j \sum_k d(k,j)\langle \varphi_0(x-k, y-j), \varphi_i(x-l, y-m)\rangle \\ &= \sum_j \sum_k d(k,j) a_{0i}(l-k, m-j) \end{aligned}$$

where the sequences $a_{0i}(k,j)$ are defined as

$$a_{0i}(k,j) = \langle \varphi_0(x-k, y-j), \varphi_i(x-l, y-m)\rangle. \tag{4}$$

These sequences also correspond to the sampled version of the cross-correlation between the output and input functions φ_0 and φ_i. In the system, the measurement values $c_i(k,j)$ are filtered by $q_i(k,j)$ and summed over $i = 1, \cdots, N$ to give us $d_f(k,j)$. Because of (2) and (3), we obtain

$$\sum_{i=1}^{N} (d * a_{0i} * q_i)(k,j) = d(k,j)$$

or

$$\sum_{i=1}^{N} (a_{0i} * q_i)(k,j) = \delta(k,j). \tag{5}$$

In the Fourier domain, (5) is expressed as

$$\sum_{i=1}^{N} A_{0i}(u,v) Q_i(u,v) = 1 \tag{6}$$

where $Q_i(u,v)$ is the Fourier transform of $q_i(j,k)$ and

$$A_{0i}(u,v) = \sum_j \sum_k \Phi_0(u-k, v-j)\bar{\Phi}_i(u-k, v-j) \tag{7}$$

with $\Phi_i(u,v)$ the Fourier transform of $\varphi_i(x,y)$, and $\bar{\Phi}$ the complex conjugation of Φ. Therefore, any set of filters that

provides a projection solution must satisfy (5) or equivalently (6).

In Appendix A, it is shown that all projection solutions are given by the class of filters

$$Q_i(u,v) = \frac{V_i(u,v)\bar{A}_{0i}(u,v)}{\sum_{j=1}^{N} V_j(u,v)|A_{0j}(u,v)|^2} \tag{8}$$

where the coefficients $V_i(u,v)$ are weighting terms that provide degrees of freedom in the filter design while enforcing the overall system projection constraint. If $\varphi_0(x,y) = \mathrm{sinc}(x)\,\mathrm{sinc}(y)$ (separable sinc), then we can show that (8) reduces to a restoration approach in microscopy [14].

For a set of projection filters, the subspace to which the projection is orthogonal is

$$V_q = \left\{ h(x) = \sum_j \sum_k \varphi_q(x-k, y-j)p(k,j) \;\middle|\; p(k,j) \in l_2 \right\}$$

where

$$\varphi_q(x-k, y-j) = \sum_{l=1}^{N} \sum_m \sum_n q_i(k-m, j-n)\varphi_i(x-m, y-n)$$

can be considered the overall input impulse response of the system. Note that while the filters q_i are discrete, the function φ_q is continuously defined.

C. Comparison to Classical Methods

While (8) specifies all solutions that are projectors into V_0, it does not necessarily correspond to a meaningful optimization problem in the spatial domain. A related problem with a more accessible interpretation in the spatial domain is to minimize the cost function

$$\min_{q_1,\cdots,q_N} \sum_{i=1}^{N} ||\mathbf{w}_i * (\mathbf{r}_i - \tilde{\mathbf{c}}_i)||^2$$

where $\mathbf{r}_i$ is a vector containing the noisy measurement values $r_i(k,j)$, $\tilde{\mathbf{c}}_i$ is a vector containing the measurement values for the case in which the system output $\tilde{f}(x,y) + \tilde{n}(x,y)$ is reapplied to the input [i.e., it passes through the input filters and is sampled; cf. Fig. 2 and (1)], and $\mathbf{w}_i$ is a weighting filter with transfer function $W_i(u,v)$. This weighting filter will typically accentuate some spectral components of the error. In the Fourier domain, the solution to the above optimization problem is

$$Q_i(u,v) = \frac{|W_i(u,v)|^2\bar{A}_{0i}(u,v)}{\sum_{j=1}^{N} |W_j(u,v)|^2|A_{0j}(u,v)|^2} \tag{9}$$

which is a subset of the collection of filters given in (8) (e.g., $V_i(u,v) = |W_i(u,v)|^2$). The above cost function measures the degree to which the estimate, $\tilde{f}(x,y)$, is consistent with the ideal measurements $c_i(k,j)$ $i = 1,\ldots,N$.

The above optimization problem can be compared to the optimization problem that leads to most classical methods including the Wiener filter. This optimization problem is

$$\min_{q_1,\cdots,q_N} ||f(k,j) - (\tilde{f}(k,j) - \tilde{n}(k,j))||^2$$

where sampling of the signals is usually performed (hence $f(k,j)$ instead of $f(x,y)$) and the criterion is to minimize the mean square error between the input signal and the output data. Thus, the noise is explicitly contained in the optimization process and the solution depends upon the power spectrum of the noise and the power spectrum of the input signal. This approach requires *a priori* information that we are assuming is not always available and that may be difficult to obtain.

Thus far, we have introduced the idea of imposing a projection constraint on the entire system by our selection of the filters $q_i(k,j)$ $i = 1,\cdots,N$. This has led to an infinite number of filters (by selection of the weight parameters) that provide a system that is a projector. At this point it is necessary to consider a criteria which will select the "best" filter set out of this family. An obvious choice for a criteria is one that considers what until now we have ignored: the system noise.

III. Optimization of Weights

Ideally, the weights $V_i(u,v)$ should be selected to reduce the noise at the system output. Previous work in this area has provided only heuristic methods for selecting the weighting terms [14]. Here, we will consider two situations. In the first, it is assumed that the power spectrum of the noise is known, while in the second case, the noise power spectrum is unknown. In both cases, the noise is assumed to be uncorrelated between channels (which is a reasonable assumption in the case of an electron microscope focal series), and the restoration filters are of the form given in (8).

A. Known Noise Power Spectrum

The power spectrum of the noise after the summation of the output of the restoration filters is

$$P_N(u,v) = \sum_{i=1}^{N} |Q_i(u,v)|^2 P_{n_i}(u,v)$$

where $P_{n_i}(u,v)$ is the noise power spectrum introduced in channel i. The goal is to minimize the output noise power which is equivalent to selecting the weights such that $P_N(u,v)$ is minimized at each frequency. From the form of (8) it is clear that if $V_i(u,v)$ $i = 1,\cdots,N$ was the optimal solution, then $\alpha V_i(u,v)$ would also be optimal. Therefore, the problem of minimizing $P_N(u,v)$ can be approached as minimize

$$\sum_{i=1}^{N} |V_i(u,v)|^2|A_{0i}(u,v)|^2 P_{n_i}(u,v)$$

with respect to $V_i(u,v)$ $i = 1\cdots,N$ subject to the normalization constraint

$$\sum_{i=1}^{N} V_i(u,v)A_{0i}(u,v) = \kappa$$

where κ is a positive constant. Minimization leads to the optimal weights

$$V_i(u,v) = \frac{1}{P_{n_i}(u,v)}.$$

It is therefore optimal to place low weight where the noise is significant.

B. Unknown Noise Power Spectrum

If the noise power spectrum is not known, one can still make a reasonable selection of the weighting terms to reduce the noise power at the output. If the system is a projection operator and the input signal is contained within the subspace defined by the reconstruction device, then reducing the system's total power output is equivalent to reducing the noise power at the output.

The reason only the noise power is reduced becomes clear when the system output is again expressed as the summation

$$\tilde{f}(x,y) + \tilde{n}(x,y)$$

where $\tilde{f}(x,y)$ is produced by the input $f(x,y)$ and $\tilde{n}(x,y)$ represents the output caused by the noise inputs $n_i(k,j)$ $i = 1, \cdots N$. If the system is a projection operator, and if $f(x,y) \in V_0$, then a change in the weights $V_i(u,v)$ will produce the same $\tilde{f}(x,y)$ (since $f(x,y) = \tilde{f}(x,y)$) but will produce a different $\tilde{n}(x,y)$. This characteristic of the projection system means that reducing the total output signal power will reduce only the output signal power caused by $\tilde{n}(x,y)$ and not $\tilde{f}(x,y)$ when $f(x,y) \in V_0$.

We would therefore like to design the filters such that the overall total power output is minimized. Let the summation of the digital filter outputs be given in the Fourier domain by

$$D(u,v) = \sum_{j=1}^{N} Q_j(u,v) R_j(u,v)$$

where $R_j(u,v) = C_j(u,v) + N_j(u,v)$ is the known measurement in channel j, $C_j(u,v)$ is the noise-free value in channel j, and $N_j(u,v)$ is the noise in channel j.

Similar to the known noise case, this problem can be expressed as

$$\min_{V_i} E\{|D(u,v)|^2\}$$

subject to the normalization constraint $\sum_{i=1}^{N} V_i(u,v)|A_{0i}(u,v)|^2 = \kappa$. This normalization is included to account for the fact that the solutions $V_i(u,v)$ and $\alpha V_i(u,v)$ $i = 1, \cdots, N$ are equivalent.

Using a matrix notation and dropping the frequency variables for simplicity, the optimal weights are given by

$$\mathbf{v} = \frac{\mathbf{Y}^{-1}\mathbf{a}}{\mathbf{a}^T\mathbf{Y}^{-1}\mathbf{a}}$$

where $[\mathbf{Y}]_{jk} = \mathrm{Re}\{\bar{A}_{0j}A_{0k}E\{R_j\bar{R}_k\}\}$, $\mathbf{a} = [|A_{01}|^2, \cdots, |A_{0N}|^2]^T$, and $\mathbf{v} = [V_1, \cdots, V_N]^T$. Details of this solution are provided in Appendix B. Due to the significant amount of noise in electron micrographs, it is necessary in practice to use regularization in estimating $E\{R_j\bar{R}_k\}$ (e.g. windowing or parametric methods [1]). Methods discussed in [16] may be of particular significance for this problem.

IV. Practical Issues

If there is an area of the frequency spectrum for which no signal information is obtained, then the projection-based approach can seriously overamplify the noise. If possible, the frequency nulls of each channel should be selected such that they are not close to one another. That is there should not be a spatial frequency u_0, v_0 for which

$$\Phi_i(u_0, v_0) \approx 0 \quad i = 1, \cdots, N.$$

In the case of electron microscopy, the frequency null locations are "placed" by adjusting the defocus setting of the microscope prior to recording the image. Careful selection of the focal settings can produce a collection of images that have no common frequency nulls. If this selection is not possible, then a clipping operation may be performed on the restoration filters prior to their use, which will avoid a boosting of the noise. Mathematically, this operation can be represented by

$$Q_{t_i}(u,v) = \begin{cases} \delta e^{j(\angle Q(u,v))}, & Q_i(u,v) > \delta \\ Q_i(u,v), & \text{else} \end{cases}$$

where the parameter δ is determined by the level of noise. This is similar to the regularization of inverse filters as described in [17]. Interestingly, for the single channel case $(N = 1)$ the filter $Q_{t_i}(u,v)$ with $\delta = 1.0$ is a commonly used restoration method in electron microscopy (assuming the only degradation being corrected is $\sin[\gamma_i(u,v)]$ [cf. (10)]. This filter amounts to simply correcting the phase reversals which occur from the degradation.

Registration of the images prior to the final summation in Fig. 2 is a nontrivial problem especially in images as noisy as those found in electron microscopy. In practice, the images must be preprocessed to enhance contrast and reduce noise. These preprocessed images are then used in a routine which determines a geometric transformation to apply to the images for registration [18], [19].

The restoration method we have described requires knowledge of the exact frequency response of the channel degradations. In many applications, these degradations must be estimated from the recorded data [20]–[26]. In the case of electron microscopy, the noise is such that there may be significant uncertainty in the estimate of the defocus parameters which define the channel responses. For the electron microscopy application, the noise-free Fourier transform of the recorded values is given by (cf. [5])

$$R_i(u,v) = H_i(u,v)(\delta(u,v) + \sin[\gamma_i(u,v)])S(u,v) \quad (10)$$

where $S(u,v)$ is the Fourier transform of the input signal and $H_i(u,v)(\delta(u,v) + \sin[\gamma_i(u,v)])$ is the frequency response of channel i, which is to be estimated; here, amplitude contrast effects have been ignored. The function $H_i(u,v)$ is a lowpass function that is produced by source coherence effects. The term $\sin[\gamma_i(u,v)]$ includes phase reversals and frequency nulls,

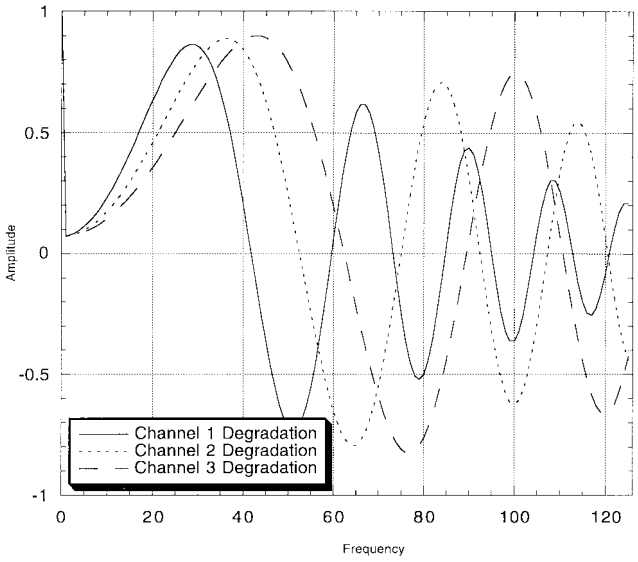

Fig. 3. Frequency response of channels.

which are a function of the microscope focal setting. For the ith channel, $\gamma_i(u,v)$ is given by

$$\gamma_i(u,v) = \frac{2\pi}{\lambda}\left[\frac{C_s(u^2+v^2)^2\lambda^4}{4} - \frac{\Delta f_i(u^2+v^2)\lambda^2}{2}\right]$$

where λ is the operating wavelength of the microscope, C_s is the spherical aberration of the objective lens, and Δf_i is the focal setting of the microscope for the ith channel. The quantity λ is determined by the voltage setting of the microscope and is known *a priori*. The spherical aberration is known *a priori* and is often provided by the microscope manufacturer. To estimate the shape of $\sin[\gamma_i(u,v)]$ $i = 1,\ldots,N$ it is necessary to determine the parameters Δf_i for $i = 1,\cdots,N$ from the recorded data.

The first step in estimating the Δf_i $i = 1,\cdots,N$ involves computing an estimate of the power spectrum of the recorded data which we denote by $|R_i(u,v)|^2$. Since the term $\sin[\gamma_i(u,v)]$ is radially symmetric (assuming minimal astigmatism), the power spectrum estimate is radially averaged. Minima of the radially averaged function $|R_i(f)|^2$ will occur near the zero crossings of the function $\sin[\gamma_i(0,v)]$. Due to the extreme noise and the effects of $H(u,v)$, it is possible that only one or two minima are distinguishable. If more nulls are visible, the defocus is determined by computing a nonlinear least squares fit between the data and a model which assumes first-order Markov properties for the signal and the noise. If only a few minima are visible, then the defocus parameter is estimated using estimated minima locations. The position of the minima are usually estimated using a local quadratic fit. Cepstral based approaches [26], [27] are not useful for estimating the defocus, since the nulls of $\sin[\gamma_i(u,v)]$ are not equally spaced. In the next section, we provide some simulation results.

V. Simulations

Here we perform a three-channel simulation in which a test image shown in Fig. 4 is degraded by

$$\Phi_i(u,v) = H_i(u,v)(\delta(u,v) + \sin[\gamma_i(u,v)]) \quad i = 1,2,3$$

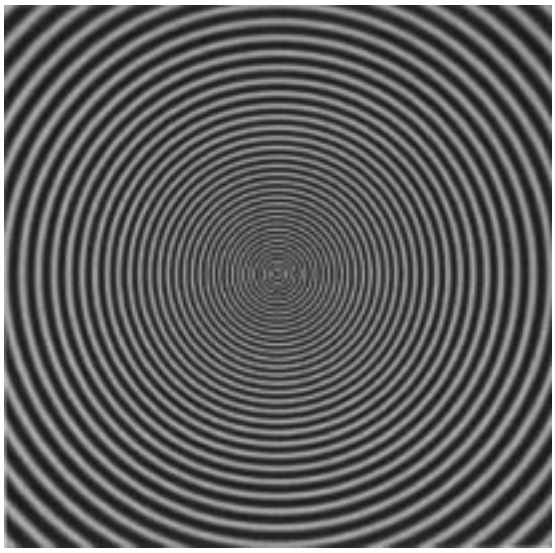

Fig. 4. Undegraded chirp image.

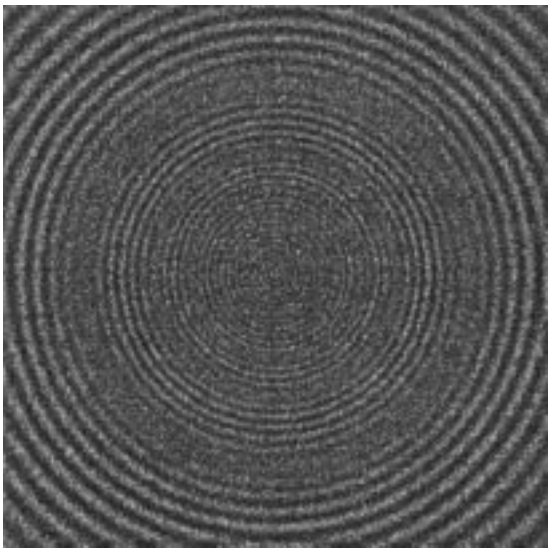

Fig. 5. Simulated recorded data for channel 1.

with $\lambda = 3.69274$ pm, $C_s = 2$ mm, $\Delta f_1 = 500$ nm, $\Delta f_2 = 700$ nm, and $\Delta f_3 = 1100$ nm, where $H_i(u,v)$ is the lowpass function produced from source coherence. $H_i(u,v)$ is exponentially decaying and depends upon the focus value, wavelength, and other known microscope parameters. The radial profile of each channel frequency response is shown in Fig. 3. A sampling rate of 0.333 nm/pixel was simulated with 256 × 256 images. White Gaussian noise was added to produce an average SNR of 0 dB. Specifically the SNR was measured as

$$\text{SNR} = 10\log\left(\frac{\sigma_1^2+\sigma_2^2+\sigma_3^2}{3\sigma_{\text{noise}}^2}\right)$$

where σ_i^2 is the variance of the noise-free degraded signal in channel i and σ_{noise}^2 is the variance of the noise added to each channel. Multiple realizations of the restored image were produced and then ensemble averaged to simulate the noise reduction achieved by combining multiple specimens. The noisy degraded outputs of each channel are shown in Figs. 5–7. The simulated chirp image is used since it demon-

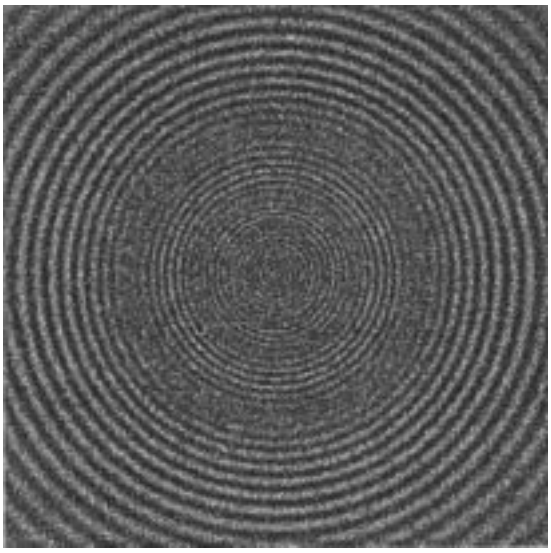

Fig. 6. Simulated recorded data for channel 2.

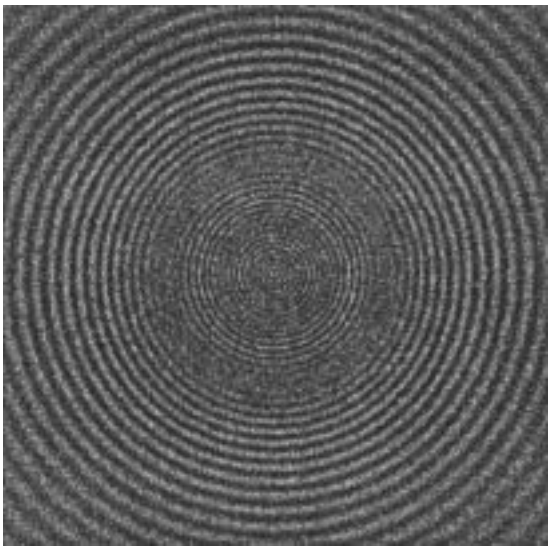

Fig. 7. Simulated recorded data for channel 3.

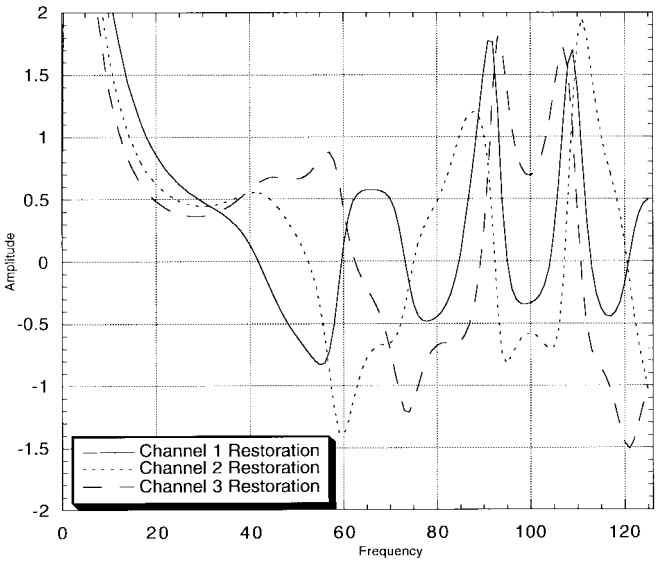

Fig. 8. Projection-based restoration filters.

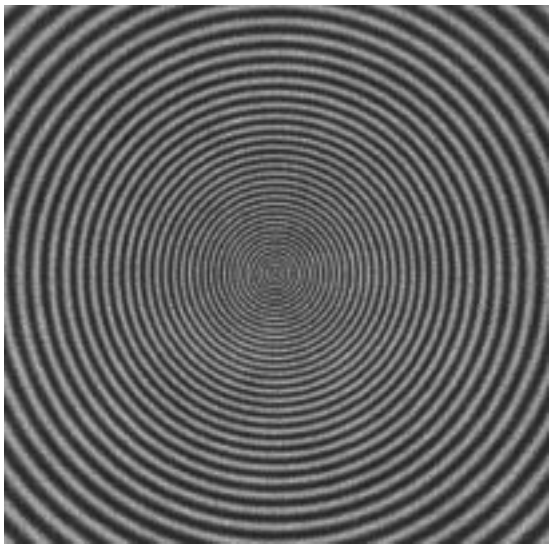

Fig. 9. Projection-based multichannel restoration using optimal weights.

strates the limitations of the restoration methods very well. Similar results are achieved with other images (e.g., Lena).

For the output space, we selected the separable sinc. In this case

$$A_{0i}(u,v) = \sum_j \sum_k \mathrm{rect}(u-k, v-j)\bar{\Phi}_i(u-k, v-j)$$
$$= \bar{\Phi}_i(u,v) \quad \text{for } |u|, |v| \le \frac{1}{2}$$

that is the $A_{0i}(u,v)$ $i = 1,2,3$ are simply bandlimited (and conjugated) versions of the degradation filters $\Phi_i(u,v)$ $i = 1,2,3$. The frequency radial profiles of the projection-based restoration filters with optimum weights for white noise, $V_i(u,v) = 1.0$, are shown in Fig. 8. The restoration using the filters in Fig. 8 is shown in Fig. 9 after the averaging over 15 realizations. The resulting residual is shown in Fig. 10. Note that the residual in Fig. 10 does not contain any signal information (i.e., $f(x,y) - (\tilde{f}(x,y) + \tilde{n}(x,y)) = \tilde{n}(x,y)$).

For comparison, we also performed a multichannel Wiener restoration [2] in which the power spectrum of the input was estimated as the periodogram of a prototype image. We put ourselves in the best possible conditions using the correct chirp image as the prototype. The optimal Wiener filter was determined by minimizing the mean square error in each individual realization. Fig. 11 shows the restoration result when using the chirp image as the prototype for 0 dB SNR with averaging over 15 realizations. As far as the high-frequency details are concerned, the result is obviously much worse as the one displayed in Fig. 9. This example exacerbates the signal distortion problem associated with some of the standard statistical methods.

In this particular simulation setting, we can obviously do better with a global Wiener solution that also takes into account the noise reduction achieved in the postprocessing averaging stage. This global solution is equivalent to the previous one if we assume that the noise variance in each individual image is divided by the number of realizations. The restoration results that are globally optimum in the Wiener sense are presented in Fig. 12. Not surprisingly, there is a much better filtering of the

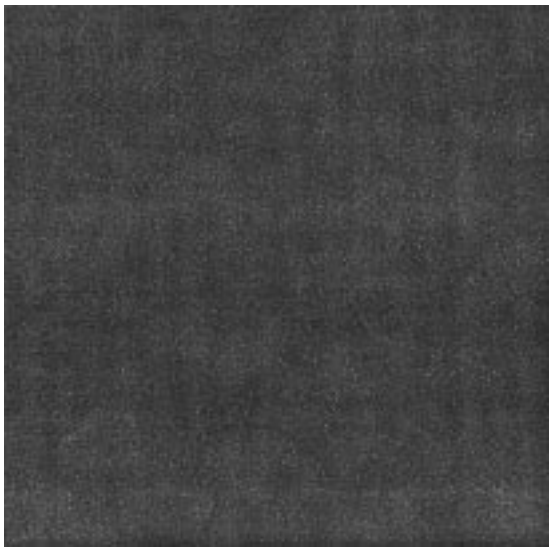

Fig. 10. Residual image for projection based restoration shown in Fig. 9.

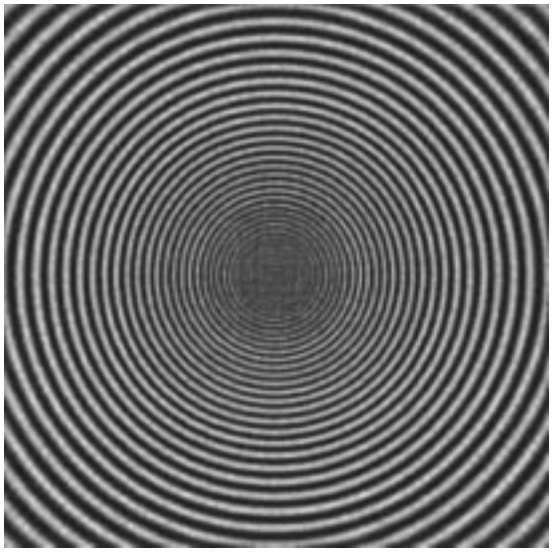

Fig. 11. Multichannel Wiener restoration using chirp image as prototype followed by an averaging over 15 realizations. The Wiener filter is optimized on an individual basis for each realization.

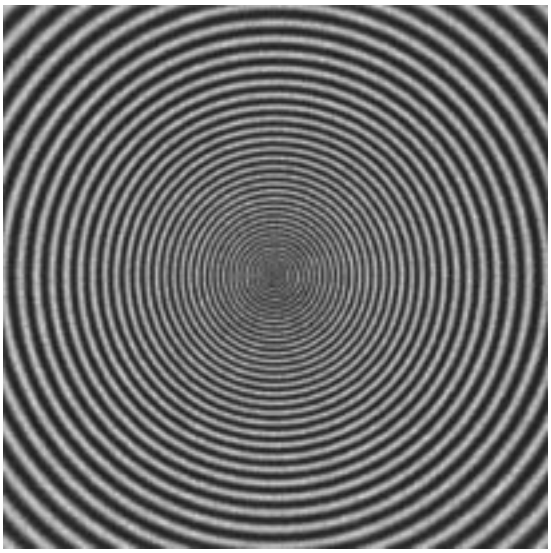

Fig. 12. Optimal multichannel Wiener restoration (minimum mean square error).

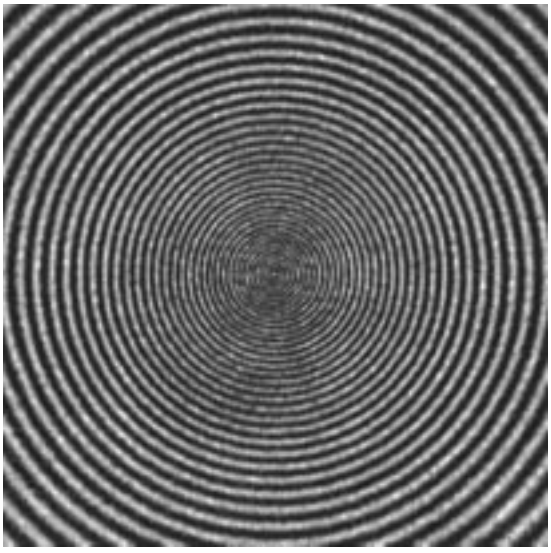

Fig. 13. Incorrect global Wiener restoration using Lena image as prototype.

noise compared to the results in Fig. 9. However, there is still some attenuation of high-frequency details and it is not entirely clear which result is the best for a human observer. In addition, as mentioned in the introduction, it may be very difficult in practice to design a Wiener filter that is globally optimum, because the exact noise reduction that will be achieved in the reconstruction phase of Fig. 1 is not known *a priori*. For the 3-D reconstruction of randomly oriented particles, this noise reduction will depend a lot on the data (which orientations are available, the type of symmetry, etc.), and on the reconstruction algorithm which is very complex [28], [29]. Moreover, the noise reduction is very unlikely to occur in a space-invariant fashion. Applying a global Wiener solution is also problematic in the simpler case of correlation averaging because it is necessary to register the individual realizations and to detect outliers prior to averaging [30]. Last, the Wiener solution is very much dependent on the *a priori* knowledge, which is typically not available in these biological applications [12]. Using prior information that is not correct may cause significant distortions. This distortion is illustrated by Fig. 13, which shows the restoration with a global Wiener filter that uses the Lena image as the prototype; the modeling of the noise is correct and accounts for the averaging performed during postprocessing.

Finally, in Fig. 14 we have provided a plot of the square error between the restoration and the original image versus the number of realizations combined. From the graph, it is clear that as the number of realizations increases, the projection based restoration approaches the optimal Wiener restoration. In addition, note that if the noise reduction achieved in the postprocessing stage is not accounted for in the Wiener filter, then there is little improvement in the restoration as the number of realizations increases. Last, for the images that we have shown (averaged over 15 realizations), note that although the projection-based restoration image has a larger square error than either Wiener restoration, the projection-based restoration image preserves all of the signal detail.

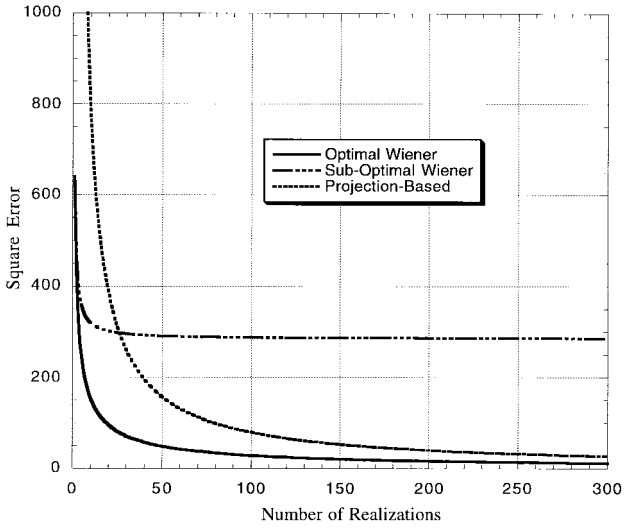

Fig. 14. Square error for projection and Wiener restorations versus number of realizations averaged.

VI. Conclusion

Unlike classical statistical-based methods, the projection based restoration preserves all of the information about the original signal when the signal is contained in the reconstruction space. In such a case, the residual will consist of noise only. This makes the method useful for applications such as electron microscopy in which noise is reduced in a postprocessing stage and for which there is little *a priori* information about the original signal or the amount of noise reduction that will be obtained in the postprocessing stage.

Appendix A

We will drop the frequency indices for clarity. First consider a set of filters of the form

$$B_i = \frac{V_i \bar{A}_{0i}}{\sum_{j=1}^{N} V_j |A_{0j}|^2}.$$

We wish to show that a filter expressed in this form will always satisfy the projection constraint given by (5), which in the Fourier domain becomes

$$\sum_{i=1}^{N} A_{0i} B_i = 1.$$

Substituting the B_i $i = 1, \cdots, N$ into the above expression immediately shows that the set of filters will produce a system which is a projection operator.

Next, we wish to show that any arbitrary set of filters P_i $i = 1, \cdots, N$ which satisfy the projection constraint $\sum_{i=1}^{N} A_{0i} P_i = 1$ can always be expressed in the form

$$P_i = \frac{V_i \bar{A}_{0i}}{\sum_{j=1}^{N} V_j |A_{0j}|^2}. \tag{A1}$$

The problem is to find a set of weights V_i $i = 1, \cdots, N$ such that the above relationship is true. A solution is to select the weights

$$V_i = \begin{cases} P_i / \bar{A}_{0i} & \bar{A}_{0i} \neq 0 \\ 0 & \bar{A}_{0i} = 0. \end{cases}$$

Substituting this solution into (A-1) leads to

$$P_i = \frac{P_i}{\sum_{j=1}^{N} P_j A_{0j}} = \frac{P_i}{1}.$$

Therefore, the filters P_i $i = 1, \cdots, N$ can be expressed in the form given in (A1).

Appendix B

Here we drop the frequency indices for clarity. The problem is to minimize

$$E\{|D|^2\} = E\left\{ \left| \sum_{j=1}^{N} Q_j R_j \right|^2 \right\} = E\left\{ \left(\sum_{j=1}^{N} Q_j R_j \right) \left(\sum_{i=1}^{N} \bar{Q}_i \bar{R}_i \right) \right\}$$

with respect to V_i $i = 1, \cdots, N$ subject to the normalization constraint

$$\sum_{i=1}^{N} V_i |A_{0i}|^2 = \kappa$$

where $Q_j = \frac{1}{\kappa} \bar{A}_{0j} V_j$. Incorporating the constraint into the cost function, differentiating with respect to V_k and setting the constant $\kappa = 1$ produces

$$2\,\mathrm{Re}\left\{ \bar{A}_{0k} \sum_{i=1}^{N} A_{0i} V_i S_{ki} \right\} = \lambda |A_{0k}|^2 \quad k = 1, \cdots, N \tag{B1}$$

where λ is the Lagrange multiplier associated with the constraint and $S_{ki} = E\{R_k \bar{R}_i\}$. Multiplying both sides of the above equation by V_k, summing over the index k, and incorporating the constraint provides a value for λ.

$$\lambda = 2 \sum_{k=1}^{N} \mathrm{Re}\left\{ \bar{A}_{0k} \sum_{i=1}^{N} A_{0i} V_i S_{ki} \right\} V_k.$$

This value is substituted back into (B1), and with algebraic manipulations we obtain the following matrix equation:

$$\mathbf{Y}\mathbf{v} = \mathbf{a}\mathbf{v}^T \mathbf{Y}\mathbf{v}$$

where $[\mathbf{Y}]_{jk} = \mathrm{Re}\{\bar{A}_{0j} A_{0k} S_{jk}\}$, $\mathbf{a} = [|A_{01}|^2, \ldots, |A_{0N}|^2]^T$, $v = [V_1, \cdots, V_N]^T$. Matrix $\mathbf{Y}$ is not guaranteed to be of full rank. If the matrix does have full rank, then the solution for $\mathbf{v}$ is

$$\mathbf{v} = \frac{\mathbf{Y}^{-1}\mathbf{a}}{\mathbf{a}^T \mathbf{Y}^{-1} \mathbf{a}}.$$

If $\mathbf{Y}$ has rank $P < N$, then using the pseudoinverse $\mathbf{Y}^{-} = \mathbf{U}\Lambda^{-}\mathbf{U}^T$ in place of $\mathbf{Y}^{-1}$ provides the solution for $\mathbf{v}$ where $\mathbf{U}\mathbf{U}^T = \mathbf{I}_{N \times N}$, $\mathbf{U}\Lambda\mathbf{U}^T$ is an eigendecomposition of $\mathbf{Y}$, Λ is a diagonal matrix with diagonal entries $[\lambda_1, \cdots, \lambda_P, 0, \cdots, 0]$, and Λ^{-} is a diagonal matrix with diagonal entries $[\lambda_1^{-1}, \cdots, \lambda_P^{-1}, 0, \ldots, 0]$.

ACKNOWLEDGMENT

The authors would like to thank F. Booy for providing practical information on electron microscopy, B. Trus for discussions on 3-D reconstruction of biological macromolecules, and P. Thevénaz for information on image registration.

REFERENCES

[1] H. J. Trussell, M. I. Sezan, and D. Tran, "Sensitivity of color LMMSE restoration of images to the spectral estimate," *IEEE Trans. Signal Processing*, vol. 39, pp. 248–252, 1991.
[2] L. P. Yaroslavsky and H. J. Caulfield, "Deconvolution of multiple images of the same object," *Appl. Opt.*, vol. 33, pp. 2157–2162, 1994.
[3] C. A. Berenstein and E. V. Patrick, "Exact deconvolution for multiple convolution operators—An overview, plus performance characterizations for imaging sensors," *Proc. IEEE*, vol. 78, pp. 723–734, 1990.
[4] N. P. Galatsanos and R. T. Chin, "Restoration of color images by multichannel Kalman filtering," *IEEE Trans. Signal Processing*, vol. 39, pp. 2237–2252, 1991.
[5] W. O. Saxton, *Computer Techniques for Image Processing in Electron Microscopy*. New York: Academic, 1978.
[6] J. Frank, A. Verschoor, and M. Boublik, "Computer averaging of electron micrographs of 40S ribosomal subunits," *Science*, vol. 214, pp. 1353–1355, 1981.
[7] H. Engelhardt, in *Methods in Microbiology*. New York: Academic, 1988.
[8] J. F. Conway *et al.*, "Visualization of three-dimensional density maps reconstructed from cryoelectron micrographs of viral capsids," *J. Struct. Biol.*, vol. 116, pp. 200–208, 1996.
[9] N. P. Galatsanos and R. T. Chin, "Digital restoration of multichannel images," *IEEE Trans. Acoust., Speech, Signal Processing*, vol. 37, pp. 415–421, 1989.
[10] X. Huang and J. Ximen, "Discussions on the multiple-input maximum a-posteriori wave-function restoration method in high resolution electron microscopy," *J. Electron Microsc. Technol.*, vol. 17, pp. 344–350, 1991.
[11] H. J. Trussell, "Notes on linear image restoration by maximizing the a posteriori probability," *IEEE Trans. Acoust. Speech, Signal Processing*, vol. ASSP-26, pp. 174–176, 1978.
[12] ———, "A priori knowledge in algebraic reconstruction methods," in *Advances in Computer Vision and Image Processing*. Greenwich, CT: JAI, 1984, pp. 265–316.
[13] M. Unser and A. Aldroubi, "A general sampling theory for nonideal acquisition devices," *IEEE Trans. Signal Processing*, vol. 42, pp. 2915–2925, 1994.
[14] N. Unwin, "Nicotinic acetylcholine receptor at 9A resolution," *J. Molec. Biol.*, vol. 229, pp. 1101–1124, 1993.
[15] M. Vetterli and J. Kovacevic, *Wavelets and Subband Coding*. Englewood Cliffs, NJ: Prentice-Hall, 1995.
[16] S. M. Kay, *Modern Spectral Estimation, Theory and Application*. Englewood Cliffs, NJ: Prentice-Hall, 1988.
[17] A. Rosenfeld and A. C. Kak, *Digital Picture Processing*. New York: Academic, 1982.
[18] P. Thévenaz, U. E. Ruttimann, and M. Unser, "Iterative multi-scale registration without landmarks," in *Proc. IEEE ICIP'95*, Washington, DC, pp. 228–231.
[19] L. G. Brown, "A survey of image registration techniques," *ACM Comput. Surv.*, vol. 24, pp. 325–376, 1992.
[20] A. M. Tekalp, H. Kaufman, and J. W. Woods, "Identification of image and blur parameters in the restoration of noncausal blurs," *IEEE Trans. Acoust., Speech, Signal Processing*, vol. ASSP-34, pp. 963–972, 1986.
[21] K. T. Lay and A. K. Katsaggelos, "Image identification and restoration based on the EM algorithm," *Opt. Eng.*, vol. 29, pp. 436–445, 1990.
[22] S. J. Reeves and R. M. Merserau, "Blur identification by the method of generalized cross-validation," *IEEE Trans. Image Processing*, vol. 1, pp. 119–123, 1992.
[23] G. Pavolvic and A. M. Tekalp, "Maximum likelihood parametric blur identification based on a continuous spatial domain model," *IEEE Trans. Image Processing*, vol. 1, pp. 496–504, 1992.
[24] A. E. Savakis and H. J. Trussell, "Blur identification by residual spectral matching," *IEEE Trans. Image Processing*, vol. 2, 1993.
[25] D. B. Gennery, "Determination of optical transfer function by inspection of frequency domain plot," *J. Opt. Soc. Amer.*, vol. 63, pp. 1571–1577, 1973.
[26] T. M. Cannon, "Blind deconvolution of spatially invariant image blurs with phase," *IEEE Trans. Acoust., Speech, Signal Processing*, vol. ASSP-24, pp. 58–63, 1976.
[27] A. E. Savakis and R. L. Easton, "Blur indentification based on higher order spectral nulls," in *Proc. Int. Symp. Optics, Imaging, and Instrumentation*, San Diego, CA, 1994, vol. 2302, pp. 168–177.
[28] R. A. Crowther, D. J. DeRosier, and A. Klug, "The reconstruction of a three-dimensional structure from projections and its application to electron microscopy," *Proc. R. Soc. Lond.*, vol. 317, pp. 319–340, 1970.
[29] R. A. Crowther, "Procedures for three-dimensional reconstruction of spherical viruses by Fourier synthesis from electron micrographs," *Philos. Trans. R. Soc. Lond.*, vol. 261, pp. 221–230, 1971.
[30] M. Unser, A. C. Steven, and B. L. Trus, "Odd men out: A quantitative objective procedure for identifying anomalous members of a set of noisy images of ostensibly identical specimens," *Ultramicroscopy*, vol. 19, pp. 337–347, 1986.

Michael J. Vrhel (M'94) was born in St. Joseph, MI, in 1964. He received the B.S. degree in electrical engineering from Michigan Technological University, Houghton, in 1987, and the M.S. and Ph.D. degrees in electrical engineering from North Carolina State University, Raleigh, in 1989 and 1993, respectively.

From 1993 to 1996, he was a National Research Council Associate at the National Institutes of Health, Biomedical Engineering and Instrumentation Program. Currently, he is the Senior Scientist at Color Savvy Systems, Ltd., Springboro, OH. His research interests include signal restoration/reconstruction, color reproduction, and wavelets.

Michael Unser (M'89–SM'94) was born in Zug, Switzerland, on April 9, 1958. He received the M.S. (summa cum laude) and Ph.D. degrees in electrical engineering in 1981 and 1984, respectively, from the Swiss Federal Institute of Technology (EPFL), Lausanne, Switzerland.

From 1985 to 1997, he was with the Biomedical Engineering and Instrumentation Program, National Institutes of Health, Bethesda, where he headed the Image Processing Group. He is now Professor of Biomedical Image Processing at EPFL. His research centers around the numerical aspects of biomedical imaging. He has a strong interest in sampling theories, multiresolution algorithms, wavelets, and the use of splines for image processing. He is the author of over 70 published journal papers in these areas.

Dr. Unser serves as an Associate Editor for the IEEE SIGNAL PROCESSING LETTERS, and is a member of the Image and Multidimensional Signal Processing Committee of the IEEE Signal Processing Society. He is also on the editorial boards of *Signal Processing*, the *Journal of Visual Communication and Image Representation*, *Pattern Recognition*, and was Associate Editor (1992–1995) for the IEEE TRANSACTIONS ON IMAGE PROCESSING. He co-organized the 1994 IEEE-EMBS Workshop on Wavelets in Medicine and Biology, and serves as conference chair for SPIE's Wavelet Applications in Signal and Image Processing, which has been held annually since 1993. He received the Dommer prize for excellence from EPFL in 1981, the research prize of the Brown-Boveri Corporation (Switzerland) for his thesis in 1984, and the IEEE Signal Processing Society's 1995 Best Paper Award (IMDSP technical area), with A. Aldroubi and M. Eden, on B-spline signal processing.